Characterising the tidal stream power resource around France using a high-resolution harmonic database

Guillou, Nicolas; Neill, Simon; Robins, Peter

Renewable Energy

Published: 01/08/2018

Peer reviewed version

Characterising the tidal stream power resource around France using a high-resolution harmonic database

Nicolas Guillou[a,*], Simon P. Neill[b], Peter E. Robins[b]

[a]*Laboratoire de Génie Côtier et Environnement (LGCE), Cerema, Direction Eau Mer et Fleuves, ER, 155 rue Pierre Bouguer, Technopôle Brest-Iroise, BP 5, 29280, Plouzané, France*
[b]*School of Ocean Sciences, Bangor University, LL59 5AB, United-Kingdom*

Abstract

Although tidal stream energy is highly predictable, the distribution of the resource varies over small spatial scales and over tidal-to-decadal time scales, requiring detailed models and accurate analysis techniques. The present study investigates the spatial and temporal variability of the tidal stream energy resource around France, using a tidal current harmonic database. The 250 m resolution tidal database covers western Brittany and the western English Channel, two regions that have strong potential for tidal array development. As well as generating a refined resource assessment for the region, a series of simplified parameters are considered to assess resource variability, both spatially and temporally. Particular attention is dedicated to variability over spring-neap time scales (resulting from M_2 and S_2 compound tides) and current asymmetry (governed by M_2 and M_4 velocities). A clear contrast in the nature of the resource is found between sites located off the Cotentin Peninsula, which exhibit low spring-neap variability and

*Corresponding author
Email address: nicolas.guillou@cerema.fr (Nicolas Guillou)

tidal asymmetry, leading to a more continuous and therefore attractive energy conversion, and sites in western Brittany, with greater variabilities over semi-diurnal and fortnightly time scales.
Keywords: spring-neap tidal variability, tidal current asymmetry, horizontal-axis turbines, Fromveur Strait, Paimpol-Bréhat, Alderney Race

1. Introduction

Technologies for tidal stream energy conversion are still in the early stages of development, although for many countries this sector has the potential to form a significant part of their future energy mix, contributing to a reduction in carbon dioxide emissions [1]. However, prior to commercial-scale deployment of tidal stream energy converters, a detailed characterisation of the ambient hydrodynamics is required to improve device design and determine optimum turbines' locations within a wider region of strong flows. Model-generated regional resource assessments are generally restricted to a reduced number of parameters, focusing primarily on the amplitudes of mean and peak tide-generated velocity and associated stream power [2, 3, 4, 5]. Whereas such resource assessments provide an initial characterisation for site selection based on the spatial distribution of resource hotspots, it is then necessary to characterise the temporal variability of the resource over semi-diurnal-to-decadal timescales.

Following this objective, advanced resource assessments have been conducted to characterise spatial and temporal variability of the resource, using tidal analysis to derive the major tidal current harmonic components from model simulations [6, 7, 8]. These large-scale investigations, mainly focusing on the northwest European shelf seas, have provided detailed insights into tidal hydrodynamics that are particularly useful for potential device developers; for example, by exhibiting the spring-neap tidal variabilities of the resource, the expected tidal asymmetry of flow and rectilinear misalignment [7], or the phase diversity between discrete potential tidal stream energy sites [8].

These studies [6, 7, 8] derived a tidal current harmonic database in order to evaluate the variability of the tidal stream energy resource beyond mean tidal conditions. The phase relationship between the principal semi-diurnal M_2 tidal current and its quarter-diurnal harmonic M_4 may thus be calculated to characterise asymmetries in energy extraction over tidal time scales [9]. Sites identified with lower spring-neap tidal variability, which is desirable for a more consistent tidal energy yield throughout the lunar cycle, can be identified by computing the ratio between current amplitudes of principal lunar M_2 and solar S_2 semi-diurnal harmonic constituents [7]. Tidal analysis can also expose regions of diurnal inequalities where consecutive tidal cycles are of unequal magnitude, and regions of lunar inequalities where consecutive spring-neap cycles vary significantly. Over longer time scales, this approach could evaluate inter-annual (or longer) variabilities in the resource, although this has not yet been investigated in the literature.

Tidal ellipses can furthermore be generated in order to determine the orientation of the flow as either rectilinear or more rotary in character [10, 11, 12]. This approach can quantify the expected reduction in power due to rectilinear misalignment, helping developers optimise device design (e.g. fixed orientation, yawing, or floating-platform turbines). Making use of established tidal current harmonic databases, rather than developing new models, has the additional advantage of increased spatial definition liable to incorporate local solutions between 1/30 and 1/60° in coastal areas [13].

Considering these aspects of resource variability, the present study investigates the benefits associated with generating a high-resolution tidal current harmonic database for tidal stream resource assessments. Our study focuses on the waters around France, where the strongest tidal currents are located off western Brittany and in the English Channel (Fig. 1). This region hosts two full-scale test sites for horizontal-axis, bottom-mounted, turbines: (1) the OpenHydro demonstration farm off Paimpol-Brehat, and (2) the Sabella device in the Fromveur Strait between the isle of Ushant and the Molène archipelago (Figs. 1 and 2). In the western English Channel, this region covers also the Alderney Race ("Raz Blanchard"), where a tidal farm of 7×2 MW horizontal-axis turbines is planned as part of the "Normandie Hydro" project (Fig. 2). This regional analysis will finally benefit from an extensive comparison with several local resource assessments in these tidal stream energy sites [14, 15, 16, 17, 18].

This investigation uses a tidal harmonic database of elevation and depth-averaged current components, covering western Brittany and the English Channel, at a consistent spatial resolution of 250 m (Section 2.1). When compared with regional investigations conducted at kilometric spatial resolutions, the 250 m resolution database used here has the potential to resolve the tidal hydrodynamics in narrow channels and in the vicinity of headlands, both locations accounting for a high proportion of the potential tidal stream energy resource [8]. For each harmonic constituent, tidal current el-

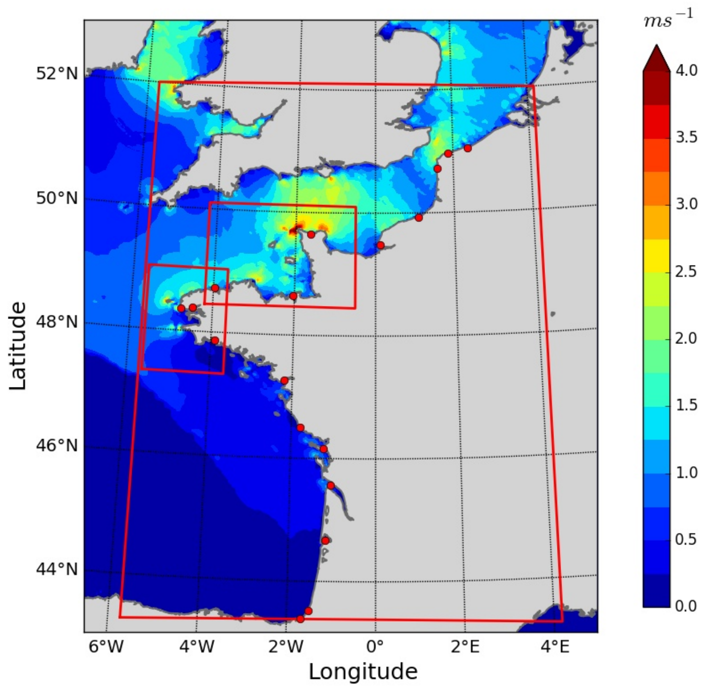

Figure 1: Maximum depth-averaged tidal current speeds during a year, recomposed from 10 primary harmonic constituents (M_2, S_2, N_2, K_2, K_1, O_1, P_1, Q_1, M_4 and MS_4), in north-west European shelf seas around France. Red lines delineate (1) computational domains over the English Channel and the Bay of Biscay and (2) high-resolution embedded domains off western Brittany and in the western English Channel. The positions of tide gauges used for the evaluation of elevation harmonic components are shown as red filled circles.

lipse parameters are derived from amplitudes and phases of eastward and northward components (Section 2.2). We also characterise variabilities in tidal stream power at quarter-diurnal and spring-neap time scales (Section 2.3). After an evaluation of the harmonic database based on a comparison between predicted and observed tidal currents (Section 3.1), the criteria adopted by Robins et al. [7], which considers peak current speeds in excess of 2.0 m s^{-1} in mean spring conditions and water depths over 25 m, is applied to identify suitable locations for the deployment of turbines in marine areas around France (Section 3.2). Particular attention is given to spring-neap tidal variability and asymmetry in power extraction (Sections 3.3 and 3.4). With respect to previous regional studies, additional investigations are finally conducted on the orientation and ellipticity of tidal currents at potential tidal stream energy sites.

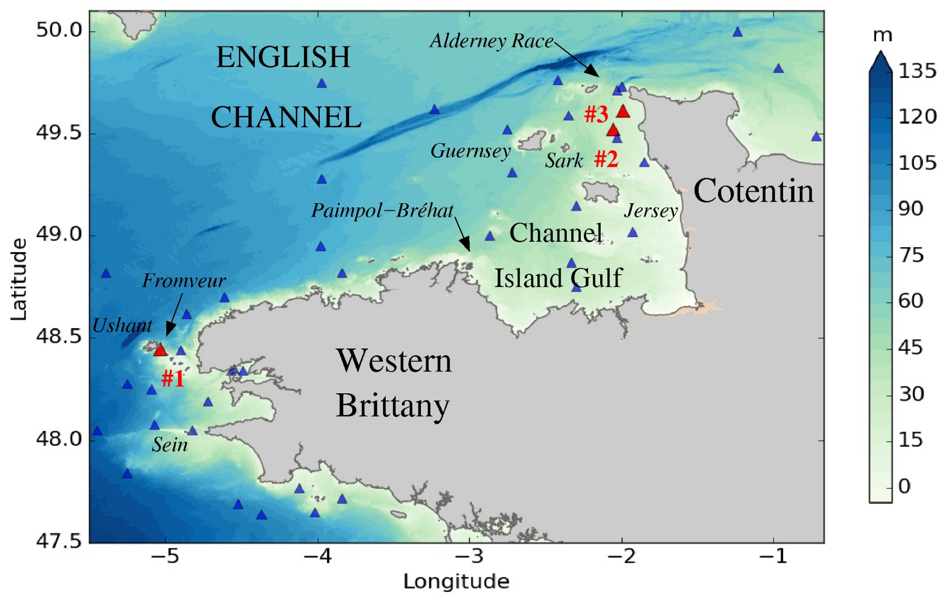

Figure 2: Bathymetry of western Brittany and the western English Channel (with respect to the lowest astronomical tide), with the locations of current meters in triangles. Blue triangles show the position of measurement points used for the assessment of MARS predictions. Red triangles (points #1, #2 and #3) correspond to locations selected, in the vicinity of major French tidal stream energy sites, for detailed evaluation of the current harmonic database.

2. Materials and methods

2.1. Tidal harmonic database

The tidal harmonic database considered here has been developed from numerical simulations with the circulation model MARS [19] applied to northwestern Europe [20]. A depth-averaged version of the numerical model covers three nested computational domains with spatial resolutions of: (1) 2 km across the northwest European shelf, (2) 700 m over the English Channel and the Bay of Biscay, and (3) 250 m in western Brittany and the western English Channel (Fig. 1). For the present investigation, we focus on outputs from the 250 m resolution coastal domains since, upon inspection of Fig. 1, these are the regions with the strongest resource. These nested models were driven by sea-surface elevations derived from tidal harmonic components developed by the French Navy SHOM ("Service Hydrographique et Océanographique de la Marine") [21], and surges predicted by the large-scale models at 2 km and 700 m spatial resolutions. Numerical simulations include atmospheric forcings from the meteorological models ARPEGE and AROME of Météo-France [22, 23], with spatial and temporal resolutions of 0.5 and 0.025^{o} and 6 and 1 hours, respectively.

Coastal predictions, at 15 min time intervals, were analysed with the Tidal Toolbox software provided by LEGOS [24], to compute the amplitude and phase of elevation and current harmonic components. These results were available on a staggered Arakawa C-grid. Bi-linear spatial interpolations were implemented to obtain all components at the center of the grid cells. As recommended by Pineau-Guillou [20], results close to offshore sea boundaries (in a band of 10% of the computational domain) were not considered in the present investigation.

2.2. Analysis of tidal currents

In the tidal database, the current of a given harmonic constituent is represented as eastward and northward components

$$\begin{cases} east & = U \cos\left(\omega t - \phi_u\right) \\ north & = V \cos\left(\omega t - \phi_v\right) \end{cases}, \tag{1}$$

where (U,V) and (ϕ_u,ϕ_v) are the associated amplitudes (m) and phases (degrees relative to Greenwich), respectively (Fig. 3), t is time (s) and $\omega = 2\pi/T$ is the angular frequency of the harmonic component with T (s) the tidal period. However, specific computational methods are required to obtain current ellipse parameters, which characterise the magnitude, orientation

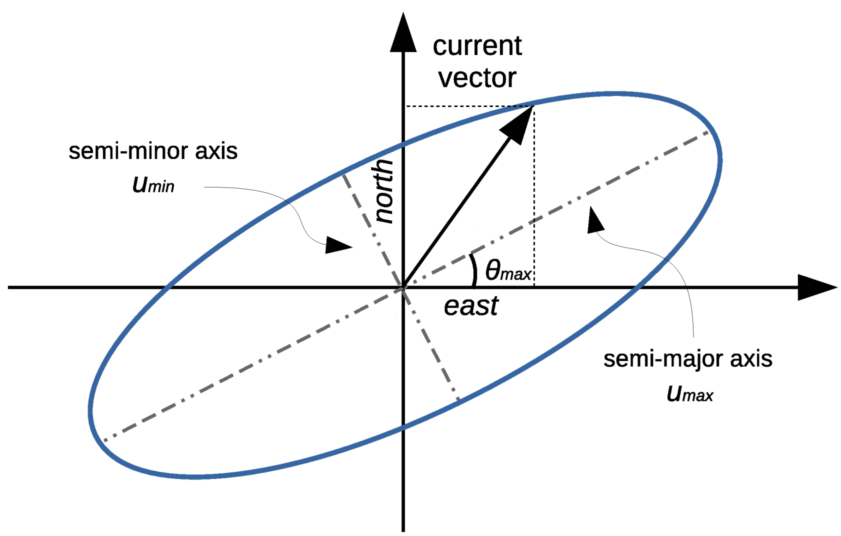

Figure 3: Schematic representation of a tidal current ellipse for a single harmonic current component with associated parameters.

and variation of associated tidal stream currents and, in turn, power. This mathematical problem may be illustrated with the approach of the ellipse semi-major axis (Fig. 3). Indeed, the amplitude of this axis, which accounts for the maximum current speed over the tidal period, cannot be directly computed from U and V, mainly as associated components are characterised by different phases ϕ_u and ϕ_v. Two methods are available to compute tidal current ellipse parameters: the first deals with trigonometric formulations, the second relies on a less intuitive parameterisation in terms of polar vectors [11]. The first method is applied here. As further details about the associated formulations are available in Pugh [11] and elsewhere, this section resumes the mathematical expression used in the present study. The maximum and minimum values of the current speed, also defined as the semi-major and semi-minor axes of the ellipse, are thus obtained from the following two equations:

$$u_{max} = \left(\frac{U^2 + V^2 + \alpha^2}{2}\right)^{1/2}, \tag{2}$$

$$u_{min} = \left(\frac{U^2 + V^2 - \alpha^2}{2}\right)^{1/2} \tag{3}$$

with $\alpha^2 = [U^4 + V^4 + 2U^2V^2 \cos(2(\phi_u - \phi_v))]^{1/2}$. The rectilinear/circular nature of the tidal current ellipse is determined from the angle:

$$\beta = \arctan\left(\frac{u_{min}}{u_{max}}\right), \tag{4}$$

which accounts for the ellipticity of the current hodograph[1]. Low values of β close to 0° indicate rectilinear currents, while values close to 45° imply

[1]A diagram that provides a vectorial visual representation of the movement of a body or a fluid.

almost circular evolutions. The tidal current vector reaches the maximum amplitude u_{max} when ωt = phase = $\phi_u - \delta \pm 180^{\mathrm{o}}$, with δ an angle obtained from the following relationship:

$$\delta = \frac{1}{2} \arctan \left(\frac{V^2 \sin(2(\phi_u - \phi_v))}{U^2 + V^2 \cos(2(\phi_u - \phi_v))} \right) . \tag{5}$$

The direction of the maximum current speed is finally given by

$$\theta_{max} = \arctan \left(\frac{V \cos(\phi_u - \phi_v - \delta)}{U \cos(\delta)} \right) . \tag{6}$$

In cases where different harmonic components are considered, this method cannot be applied, and requires the extraction of the maximum value of the recomposed time series of the tidal current over a duration compatible with the tidal periods integrated.

2.3. Tidal energy resource metrics

Following the study of Robins et al. [7] at the scale of the northwest European shelf seas, a series of parameters are considered here to characterise spatial and temporal variabilities of tidal currents and associated stream power in coastal areas around France. Attention is primarily given to the variability of tidal currents at fortnightly and semi-diurnal time scales, setting aside analysis on diurnal inequalities, which appear to be of reduced influence in western Brittany and the western English Channel [7] (Section 3.2). The tidal current harmonic components analysed describe the spring-neap tidal variability of the resource and the asymmetry of tidal currents between the flood and ebb phases of the tidal cycle.

At potential tidal stream energy sites, minimal differences between spring and neap currents are considered desirable, as this leads to a more consistent energy yield over the fortnightly spring-neap period. Tidal kinetic energy converters, designed to operate over a restricted range of velocities [25], do not appear to be adapted to hydrodynamic environments with high spring-neap tidal variability. Following Robins et al. [7], this variability is here characterised by the ratio R_{var} between the maximum amplitudes of the principal lunar M_2 and solar S_2 depth-averaged velocities, $u_{max}(\mathrm{M}_2)$ and $u_{max}(\mathrm{S}_2)$:

$$R_{var} = 1 - \frac{u_{max}(\mathrm{S}_2)}{u_{max}(\mathrm{M}_2)} \ . \tag{7}$$

Over the northwest European shelf seas, as the amplitude of S_2 velocities are always weaker than the principal M_2 velocities, R_{var} varies between 0 and 1. Values of R_{var} close to unity account for reduced spring-neap tidal variability, whilst values close to zero show noticeable differences between the spring and neap tidal cycles. Particular attention is furthermore devoted to the modifications of current directions between simple M_2 components and combined M_2 and S_2 harmonic constituents. Following Lewis et al. [26], this influence is exhibited by characterising misalignment between the flood and ebb current directions during mean spring conditions:

$$\theta_{var} = \arccos\left(\frac{-\vec{u}_{flood}.\vec{u}_{ebb}}{|\vec{u}_{flood}|.|\vec{u}_{ebb}|}\right) \tag{8}$$

where $\vec{u}_{flood}$ and $\vec{u}_{ebb}$ are the peak velocity vectors during flood and ebb periods at the location considered during mean spring conditions resulting from M_2 and S_2 harmonic components. Low values of θ_{var} characterise a reduced asymmetry in current direction, whereas higher values account for a strong tidal current misalignment.

At the semi-diurnal time scale, current asymmetry is another key parameter which characterises the variability in power production between flood and ebb. As inferred by Pingree and Griffiths [27] and Friedrichs and Aubrey [28], asymmetry in tidal currents may arise from the phase relationship between the principal semi-diurnal M_2 and its first quarter-diurnal M_4 harmonic. Adopting the parameterisation described in Section 2.2, maximum asymmetry is thus obtained when peak velocities of harmonic current vectors appear at the same time, which results in the following relationship: $\gamma = 2\mathrm{phase}(\mathrm{M}_2) - \mathrm{phase}(\mathrm{M}_4) = 0^{\circ}$ or 180° in the range $[0, 360^{\circ}]$. Symmetry of tidal currents occurs when M_2 and M_4 constituents are out of phase with $\gamma = 90^{\circ}$ or 270°. As the ratio between semi- and quarter-diurnal tidal current amplitude directly exacerbates this asymmetry, a parameter based on Robins et al. [7], is adopted here relying on ellipse characteristics:

$$A_1 = \frac{u_{max}(\mathrm{M}_4)}{u_{max}(\mathrm{M}_2)}|\cos(\gamma)| \ . \tag{9}$$

High values of A_1 in the range [0,1] account for significant tidal asymmetry, whilst low values indicate more symmetrical currents. In order to ascertain the reliability of this parameter, a comparison is performed with a more classical approach of tidal current asymmetry based on the ratio of peak tidal currents, resulting from M_2 and M_4 components, during flood and ebb:

$$A_2 = 1 - \frac{u_{peak,1}}{u_{peak,2}} \tag{10}$$

where $u_{peak,2}$ is the maximum of the peak velocity between flood and ebb and $u_{peak,1}$ is the minimum peak velocity. This parameter, which varies between 0 and 1, should therefore be consistent with A_1.

3. Results and discussion

3.1. Validation of the tidal harmonic database

The harmonic database has been assessed by Pineau-Guillou [20] by comparing recomposed tidal water elevations with observations at a series of 18 harbours along the coasts of France (Fig. 1). The root mean square error (RMSE) between predictions and observations was calculated, on average, at around 20 cm, matching with the range of mean surges. Maximum RMSE of 27 cm is obtained at Boulogne-sur-Mer in the Dover Strait (eastern English Channel). These evaluations have been extended by comparing predicted and observed harmonic components of surface elevations. The spatial distribution of major elevation components M_2 and S_2, at tide gauges, is thus approached with differences less than 5% for amplitude and 8^o for phase. Further details about the evaluation of the elevation harmonic database are available in Pineau-Guillou [20].

Coastal current predictions of MARS, used to establish the harmonic database (Section 2.1), have been compared with observations compiled by the French Navy SHOM, measured during spring tide conditions, at a series of 37 locations over western Brittany and the western English Channel (Fig. 2) [29]. In addition, the validation has been extended to include a series of three available ADCP deployments in two areas with strong potential for the exploitation of the tidal kinetic energy resource: the Fromveur Strait and the Alderney Race. These observations include (see Fig. 2 and Table 1): (1) long-term records conducted by SHOM in western Brittany (point #1), and (2) two short-term campaigns implemented by Bailly du Bois [30] in the western English Channel (points #2 and #3).

In relation to the availability of in-situ data, the validation in western Brittany was performed at 10 m above the seabed – this elevation corresponds to the operating height of proposed horizontal axis turbines in French tidal stream energy sites (Fig. 4). Following Guillou and Thiébot [17], the tidal currents at 10 m above the seabed were obtained from the recomposed depth-averaged currents by assuming a vertical logarithmic velocity profile with a bottom roughness parameter set to $z_0 = 20$ mm. Whereas a Strickler law is adopted in the depth-averaged MARS model [29], this roughness value of $z_0 = 20$ mm, adopted over bottom rock outcrops in the Fromveur Strait, provided the best estimates of current amplitude and direction at point #1 [17]. Depth-averaged currents are recomposed from the 10 primary harmonic components: M_2, S_2, N_2, K_2, K_1, O_1, P_1, Q_1, M_4 and MS_4. In spite of a tendency to overestimate spring current magnitudes, seemingly associated with different parameterisations of bottom friction, and exhibited by the positives values of the mean relative difference $\mathrm{DIFF}_{\mathrm{rel}}$ (Tab. 2), the numerical results reproduce the variations of tidal velocity, in particular, the abrupt changes between south-west and north-east directions (Fig. 4).

The evaluation of depth-averaged current amplitude in the western English Channel (Fig. 5) confirms the ability of the coastal harmonic database to characterise tidal velocities, with RMSE restricted to 0.16 $\mathrm{m\,s^{-1}}$. Further, variation of current direction is estimated with an index of agreement RE [31] over 0.98 at both measurements points #2 and #3. Stronger differences, obtained at point #3, may be associated with tidal recirculations in the vicinity of surrounding headlands that are not fully resolved in the model.

Finally, additional investigations show that the recomposed maximum depth-averaged velocities based on M_2 and S_2 components, i.e. the mean spring peak currents (Fig. 6), are consistent with current maps established by the SHOM and EDF R&D over western Brittany and the western English Channel [32], identifying areas of strong velocity amplitudes with differences restricted to 0.2 $\mathrm{m\,s^{-1}}$.

Table 1: Details of ADCP deployments.

Measurement points	Coordinates Lon.	Lat.	Water depths (m)	Periods of measurements
#1	5.036° W	48.449° N	53	19/03/1993 → 02/04/1993
#2	2.055° W	49.522° N	29	10/08/2003 → 12/08/2003
#3	1.993° W	49.614° N	25	09/08/2003 → 11/08/2003

Table 2: Statistical parameters for the evaluation of observed currents amplitude U and direction Dir at points #1, #2 and #3: the mean relative difference $\mathrm{DIFF_{rel}}$, the root mean square error RMSE and the index of agreement RE [31].

Measurement	U			Dir		
points	$\mathrm{DIFF_{rel}}$	RMSE	RE	$\mathrm{DIFF_{rel}}$	RMSE	RE
#1	0.18 $\mathrm{m\,s^{-1}}$	0.31 $\mathrm{m\,s^{-1}}$	0.96	−6.7°	36.0°	0.96
#2	0.06 $\mathrm{m\,s^{-1}}$	0.09 $\mathrm{m\,s^{-1}}$	0.97	2.1°	19.3°	0.99
#3	0.10 $\mathrm{m\,s^{-1}}$	0.16 $\mathrm{m\,s^{-1}}$	0.96	−5.7°	24.7°	0.98

3.2. Identification of potential tidal stream energy sites

In the majority of resource assessments around the United Kingdom [7, 26, 33, 34], the identification of potential tidal stream energy sites is mainly based on current speeds and water depths, neglecting further constrains associated with the practical, political, or environmental issues or

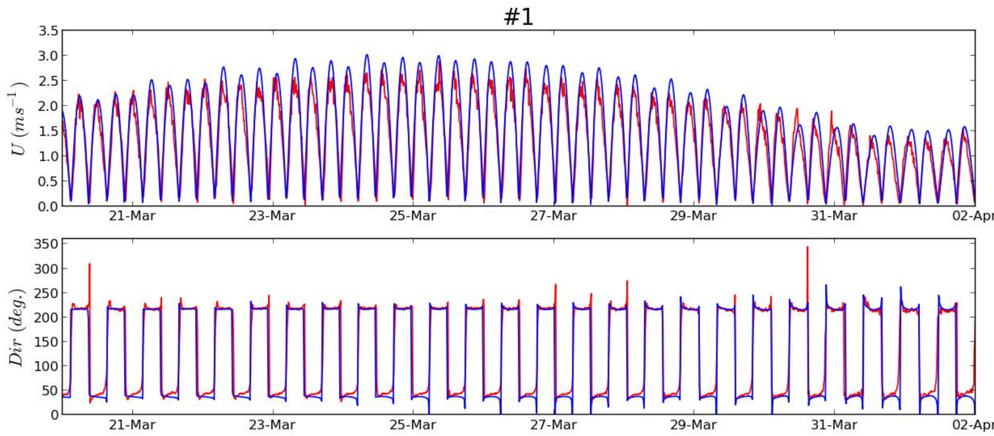

Figure 4: Recomposed (blue line) and observed (red line) time series of current amplitude and direction (anticlockwise convention from the East) 10 m above the seabed at point #1 in March-April 1993.

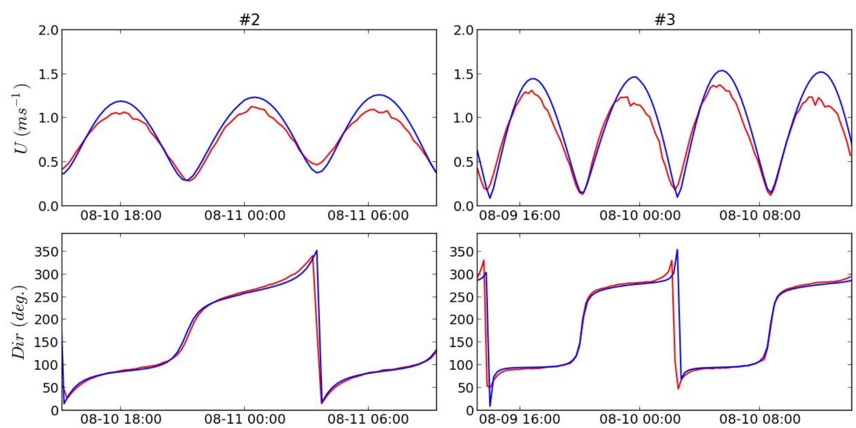

Figure 5: Recomposed (blue line) and observed (red line) time series of depth-averaged current amplitude and direction (anticlockwise convention from the East) at points #2 and #3 in August 2003.

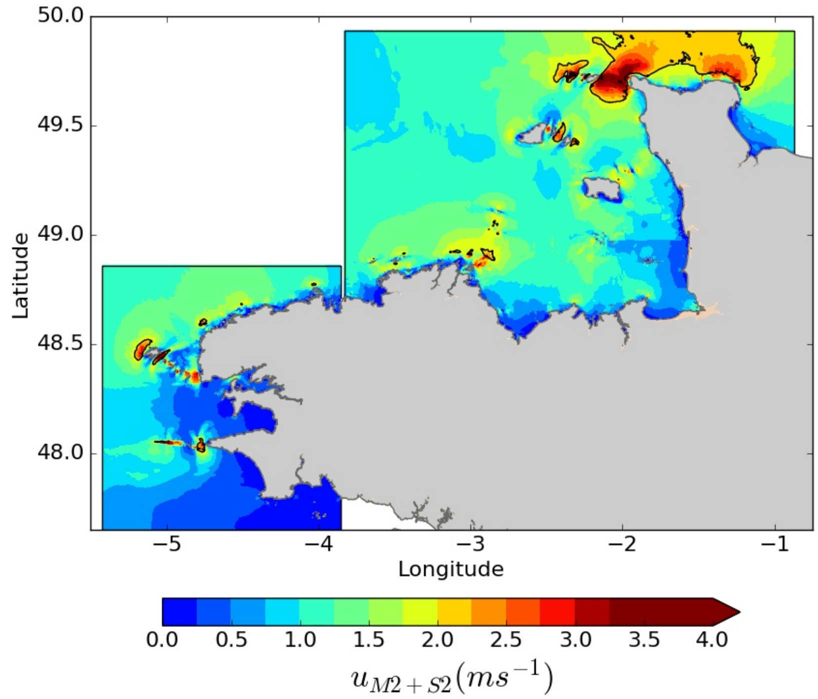

Figure 6: Maximum depth-averaged velocities from M_2 and S_2 harmonic components in western Brittany and the western English Channel. The black contours delineate potential tidal stream energy sites characterised by mean spring peak velocities over $2\ \mathrm{m\,s^{-1}}$ and water depths over 25 m.

marine activities. The present resource assessment is based on the criteria adopted by Robins et al. [7] to identify potential locations for first- and second-generation technologies of tidal stream energy converters, covering both existing prototype devices in pre-commercial demonstration and at the early stages of technology readiness [34]. This corresponds to areas with: (1) peak current speeds in excess of $2.0\ \mathrm{m\,s^{-1}}$ in mean spring conditions, and (2) a minimum water depth of 25 m. Further insights may be provided about these limits from a rationale based on the output power formula of horizontal-axis turbines $P_{out} = (\rho C_p \pi D^2 u^3)/8$ with ρ the density of sea water (kg m^{-3}), C_p the power coefficient, D the blade diameter (m) and u the tidal current speed (m s^{-1}).

Taking into account a range of device power coefficients [25], it is thus necessary to have a peak current speed of at least 2.0 m s^{-1} in combination with a minimum turbine diameter of 20 m to attain a power output of 0.5 MW, the lowest threshold of most horizontal-axis turbines currently tested and implemented at potential tidal stream energy sites (Fig. 7). The minimum current speed is 2.5 m s^{-1} to attain a power output of 1 MW with the same device characteristics. In order to ensure a constant immersion of devices and sufficient navigational clearance, a minimum water depth of around 25 m is required for this type of tidal stream power extraction.

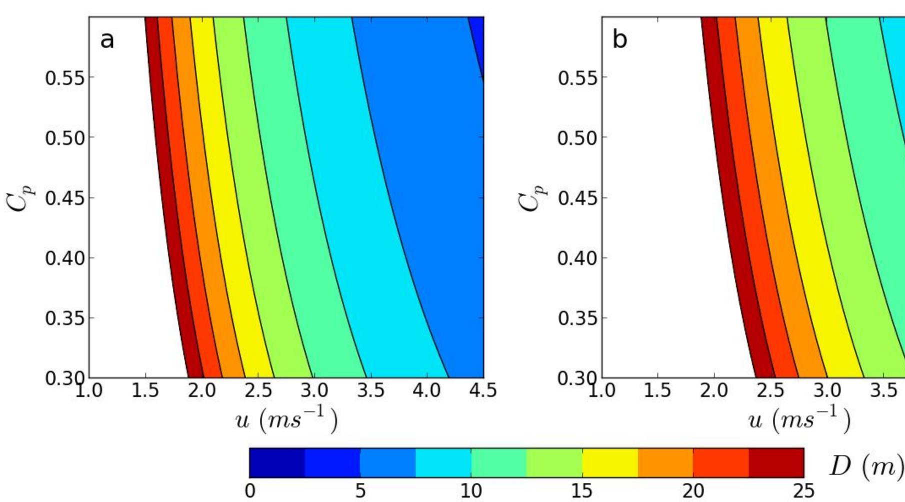

Figure 7: Minimum turbine diameter required to achieve power outputs of (a) 0.5 and (b) 1 MW, with respect to power coefficient C_p and tidal current velocity u. Diameters over 25 m are not shown on the figure.

In the present study, the criteria adopted for site selection considers the mean spring peak velocities resulting from M_2 and S_2 harmonic current components in the high-resolution coastal database (Section 2.1), and the water depth extracted from the HOMONIM ("Historique, Observation, MOdélisation des NIveaux Marins", SHOM, Météo-France) database [35, 36] which covers the areas of interest at a spatial resolution of 111 m.

Along the coasts of France, potential tidal stream energy sites are mainly identified in western Brittany and the western English Channel (Fig. 6). Whereas all sites are characterised by a mean kinetic power density that exceeds $0.8\ \mathrm{kW\,m^{-2}}$ during a mean spring tidal cycle, the western area of Alderney (Casquets), the Alderney Race and the Fromveur Strait are the three locations where this power density significantly exceeds $2.5\ \mathrm{kW\,m^{-2}}$ – meeting the resource criteria adopted by the Carbon Trust [37] for the deployment of first-generation turbine devices (Fig. 8, Table 3). The refined calculation of kinetic power density over these regions appears consistent with predictions from high-resolution nested numerical models. These results show: (1) in the Fromveur Strait, zones of high energy formed in between the islands with peak power density in each zone ranging from $4\ \mathrm{kW\,m^{-2}}$ to over $7\ \mathrm{kW\,m^{-2}}$ [16, 17], and (2) in the Alderney Race, a concentration of tidal stream energy over $10\ \mathrm{kW\,m^{-2}}$ around the Cotentin Peninsula [15, 18]. Areas identified off the Cotentin Peninsula and in the Alderney Race are particularly remarkable, accounting for a total surface of around $1750\ \mathrm{km^2}$ in the embedded coastal domain. The mean power density associated with this potential sea space is estimated at $1.6\ \mathrm{kW\,m^{-2}}$, with minimum and maximum values of 0.9 and $12.4\ \mathrm{kW\,m^{-2}}$, respectively. However, the total surface is

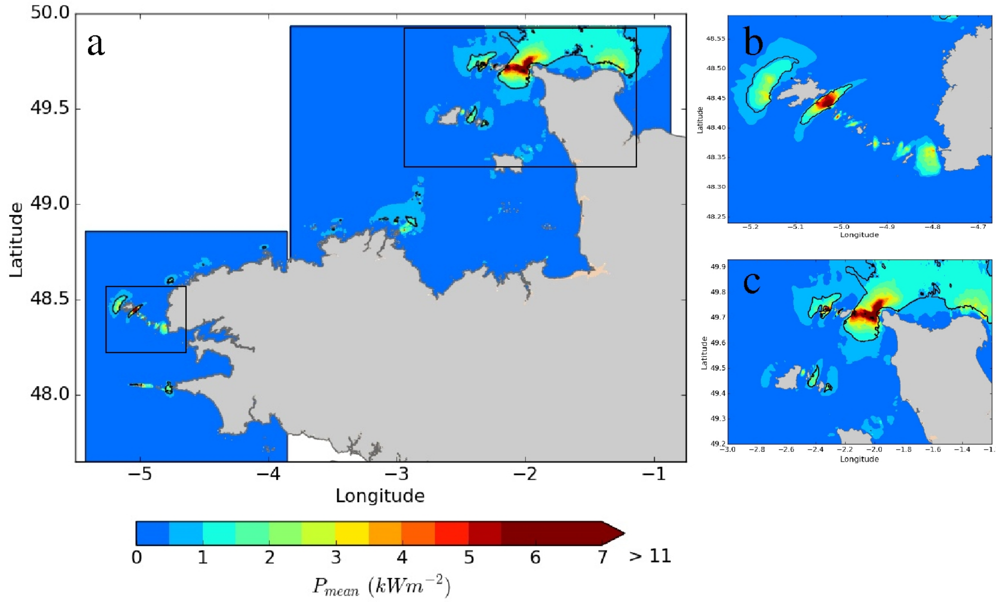

Figure 8: Mean kinetic power density distribution during a spring-neap tidal cycle (T=14.765 days)) resulting from M_2 and S_2 components in (a) coastal domains, with magnified views in (b) the Fromveur Strait and (c) the Alderney Race. The black lines delineate potential tidal stream energy sites identified in Fig. 6.

markedly reduced by 80% to 350 km^2 if a threshold of mean spring peak velocity of 2.5 $\mathrm{m\,s^{-1}}$ is imposed. This difference highlights, in particular, the increased sea space associated with the development of tidal stream turbine technologies more suited to harnessing less energetic tidal streams. It should finally be noted that the area located west of Alderney (Casquets) accounts for a total surface of 90 km^2, with averaged power density during a mean spring tidal cycle liable to exceed 9 $\mathrm{kW\,m^{-2}}$ (Table 3).

Outside of these significant areas, potential tidal stream energy sites occupy surfaces restricted to 40 km^2 – predominantly in the vicinity of headlands and straits, confirming previous investigations conducted by Neill et

Table 3: Characteristics of major potential tidal stream energy sites associated with the averaged kinetic power distribution during a spring-neap tidal cycle resulting from M_2 and S_2 components (Fig. 8): total surface, mean power density P_{mean}, minimum and maximum values of the averaged power density P_{min} and P_{max} over the sea space of tidal stream energy sites.

Sites	Areal extent (km^2)	P_{mean} ($kW\,m^{-2}$)	P_{min} ($kW\,m^{-2}$)	P_{max} ($kW\,m^{-2}$)
Raz of Sein	15	1.4	0.9	2.8
West of Ushant	40	1.4	0.8	3.2
Fromveur Strait	17	2.9	0.9	7.9
North-western Brittany	7	1.1	0.9	1.7
Paimpol-Bréhat	18	1.1	0.9	1.8
East of Sark	8	1.4	0.9	2.6
East of Guernsey (Big Roussel)	26	1.5	0.9	2.3
West of Alderney (Casquets)	90	1.5	0.9	9.9
Off Cotentin Peninsula	1753	1.6	0.9	12.4

al. [8]. Over these areas, the mean value of the associated power density is estimated between 1.1 and 1.5 $kW\,m^{-2}$ with peak values below 3.2 $kW\,m^{-2}$ (Table 3). These locations include the well-known French tidal stream energy sites in the Raz of Sein and off Paimpol-Bréhat, and also potential locations to the west of Ushant island and to the east of Guernsey (Big Roussel). In the Channel Islands Gulf, our resource assessment confirms conclusions from reports commissioned by the Carbon Trust [33, 38]. However, potential sites off the northwest coast of Guernsey and off the northeast coast of Jersey were not identified here. This is consistent with results obtained by Coles et al. [18] with a depth-averaged tidal circulation model covering these areas with a mesh resolution of 250 m. Other potential tidal stream energy sites with surfaces areas less than 8 km^2 are also identified along the northern coast of western Brittany and to the east of Sark. Over these two regions, the mean power density is estimated at 1.1 and 1.4 $kW\,m^{-2}$, respectively (Table 3).

We investigated the rectilinear/circular nature of tidal currents by focusing on the ellipticity associated with the principal lunar semi-diurnal component M_2 (Fig. 9). In the English Channel, the spatial distribution of parameter β (Eq. 4) appears consistent with the numerical investigation conducted by Fornerino and Le Provost [10], indicating strong gyratory currents in the areas surrounding Guernsey and Jersey. However, with the exception of sites identified in the Raz of Sein and to the west of Alderney, the values of β for M_2 were less than 5^o at potential tidal stream energy sites. This means that these sites contain near rectilinear M_2 tidal currents, a key property required for the installation of horizontal-axis turbines with a fixed orientation.

Finally, the capacity factor of a series of horizontal-axis turbines varying in rated power is evaluated in order to provide potential developers further insights into device operating times (Fig. 10). Indeed, the capacity factor accounts for the fraction of the year the turbine generator is operating at rated power. Capacity factor was thus computed, defined as the averaged power produced over a year divided by the rated turbine power. This analysis relies on velocities recomposed from the 10 primary tidal harmonic components used to calculate Fig. 1. The power curves considered are based on the OpenHydro device [39], by assuming a cut-in speed of 0.7 $m\,s^{-1}$ and rated speeds of 1.7, 2.1, 2.5 and 2.7 $m\,s^{-1}$, matching rated powers of 0.5, 1.0, 1.5 and 2.0 MW, respectively. The capacity factor of 0.5 MW devices exceeds 40% in most potential tidal stream energy sites, with maximum values over

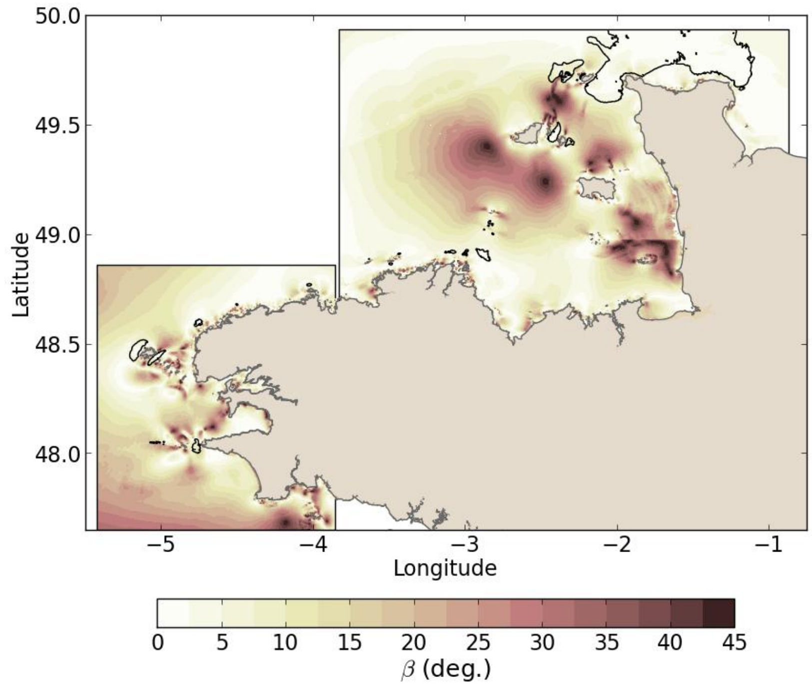

Figure 9: Spatial distribution of angle β (Eq. 4), characterising the ellipticity of M_2 tidal currents in western Brittany and the western English Channel. The black lines delineate potential tidal stream energy sites identified in Fig. 6.

70% in the Fromveur Strait, the Alderney Race and west of Alderney in relation to higher current speeds (Fig. 10-a). The capacity factor is naturally reduced for higher rated powers with values restricted to 35% for 1.5 MW turbines in most potential locations, with exceptions in the three sites previously identified (Fig. 10-c). However, the associated averaged power is found to increase for high rated power. In the Alderney Race, the averaged power produced over a year is thus restricted to 0.3 MW for 0.5 MW devices, whereas it would exceed 1.1 MW for 2 MW turbines.

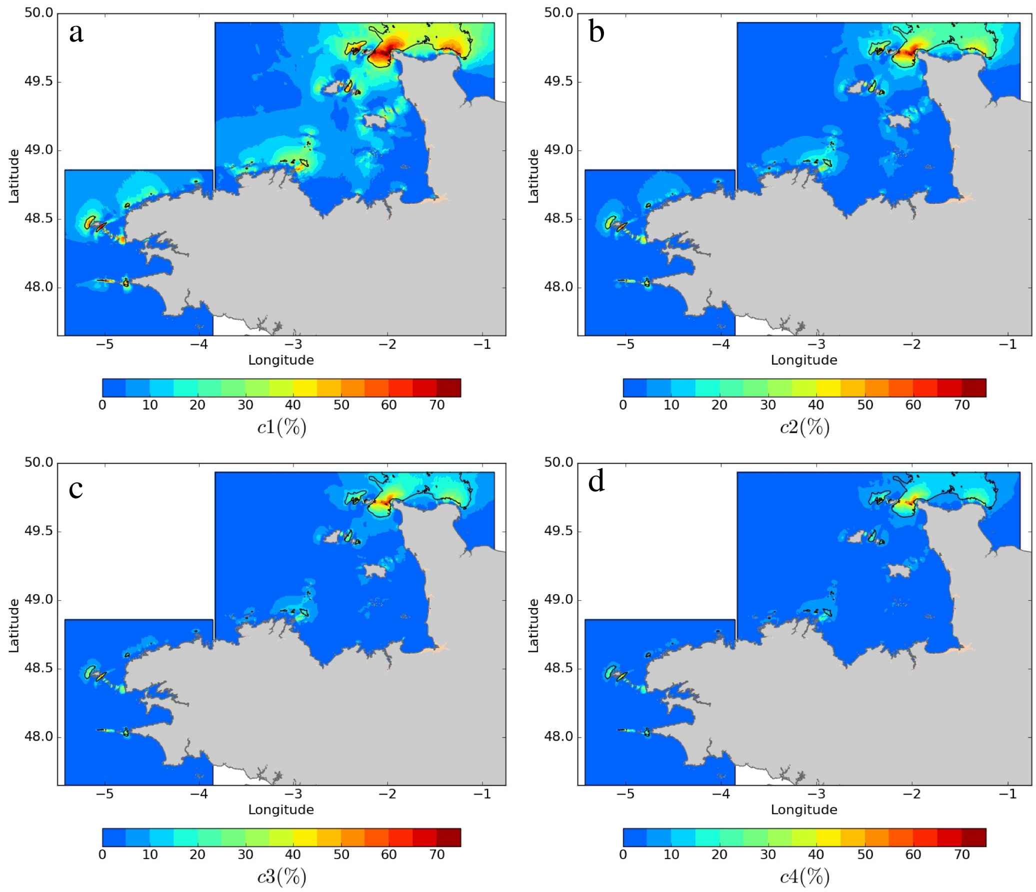

Figure 10: Annual capacity factor based on power curves with rated powers of (a) 0.5, (b) 1.0, (c) 1.5 and (d) 2.0 MW. The black lines delineate the potential tidal stream energy sites identified in Fig. 6.

3.3. Spring-neap variability

Confirming the investigation conducted by Robins et al. [7] over the north-west European shelf seas, R_{var} (Eq. 7) varies between 0.55 and 0.80 in western Brittany and the western English Channel (Fig. 11). A clear gradient of the spring-neap tidal variability of currents is exhibited in the Channel Islands between a south-western area characterised by high variability ($R_{var} < 0.61$) and a north-eastern region with reduced variability ($R_{var} > 0.67$). This difference is exhibited between the Alderney Race and the Fromveur Strait by retaining two locations with contrasting values of $R_{var} = 0.629$ in the Fromveur Strait (point p1) and $R_{var} = 0.695$ in the Alderney Race (point p2).

Fig. 12 displays the extracted depth-averaged velocities resulting from M_2 and S_2 harmonic components and the generated "technical" resource by applying the power curve of a 1.5 MW OpenHydro device and by neglecting turbine interactions and feedback between energy extraction and the hydrodynamics. While the tidal velocity reaches slightly stronger magnitudes at the location considered in the Fromveur Strait ($u_{max} = 3.41\ \mathrm{m\,s^{-1}}$ at point p1 against $3.36\ \mathrm{m\,s^{-1}}$ at point p2), currents generate less power than at the point retained in the Alderney Race. The generated power over a mean spring-neap tidal cycle is thus estimated at 223 MWh at point p1 while it reaches 235 MWh at point p2. Whereas this difference accounts for about 5% of the total spring-neap generated power, with capacity factors estimated at 42.1 and 44.2%, differences between sites increase significantly during neap tide conditions. Indeed, both locations show maximum spring tidal current velocities over the rated speed of the OpenHydro device, with differences in generated power mainly attributed to neap conditions. During neap tides, the maximum generated power is thus estimated at 0.63 MW at point p2, while it is restricted to 0.43 MW at point p1 (Fig. 12).

Further investigations, conducted to calculate tidal current misalignment, depict low values of the parameter θ_{var} (Eq. 8); restricted to 2° between the flood and ebb current directions of peak mean spring currents, in the majority of potential tidal stream energy sites. Such misalignment direction lies below the limit under which power reductions may be apparent for horizontal-fixed

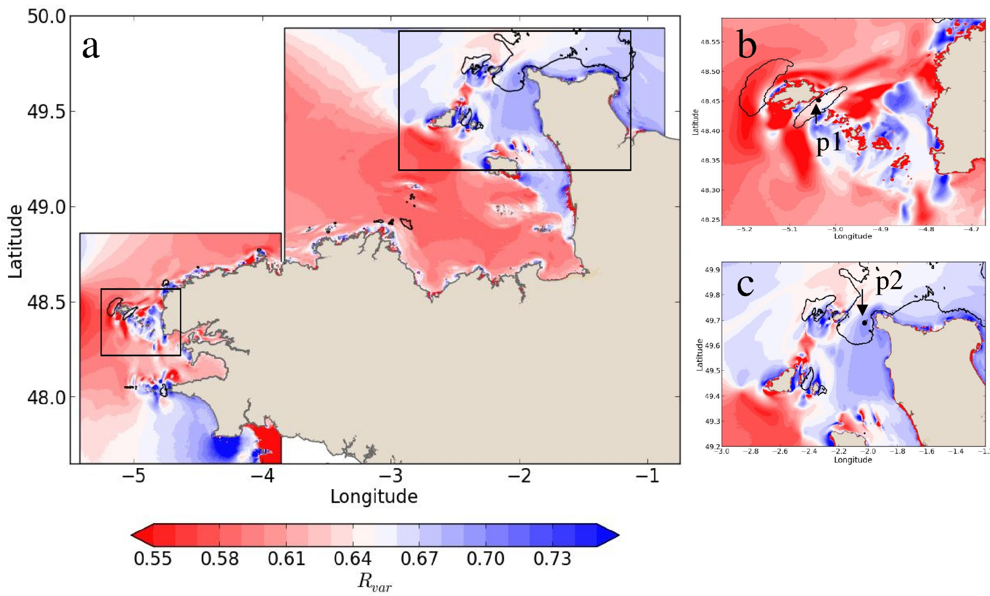

Figure 11: Spatial distribution of parameter R_{var}, characterising the variability of tidal current amplitude over a mean spring-neap cycle in (a) coastal domains, with magnified views in (b) the Fromveur Strait and (c) the Alderney Race. The black circles in (b) and (c) show the positions of points p1 and p2 used for the extraction of recomposed currents amplitude and direction (Fig. 12). The black lines delineate potential tidal stream energy sites identified in Fig. 6.

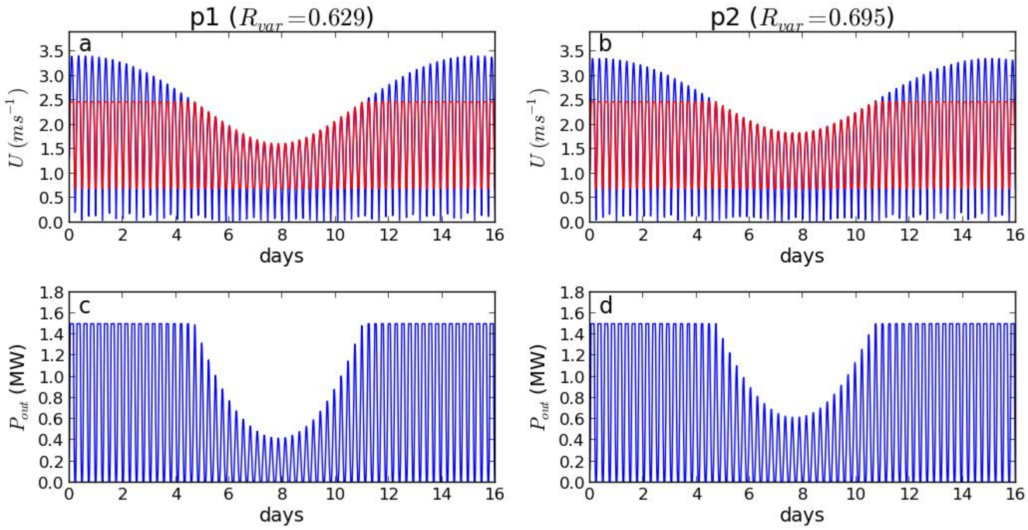

Figure 12: Predicted depth-averaged tidal current velocities U over a mean spring-neap-spring cycle, and associated generated practical power, P_{out}, based on the 1.5 MW Open-Hydro power curve in (top) the Fromveur Strait (point p1, $R_{var} = 0.629$) and (bottom) the Alderney Race (point p2, $R_{var} = 0.695$). The red line accounts for the effective tidal velocity which generates power.

axis turbines. Indeed, Galloway et al. [40] estimated this limit at 7.5^o by relying on experimental data and a Blade Element Momentum (BEM) code. More recently, Frost et al. [41] demonstrated, from Computational Fluid Dynamics modelling, a drop of 7% in the maximum theoretical available power between misalignment angles of 0 and 10^o. Directional asymmetry exceeds 15^o in limited locations of potential tidal stream energy sites. Confirming the investigation conducted by Lewis et al. [26] in the Irish Sea, this concerns mainly areas associated with tidal recirculations appearing around Cap de la Hague (the north-western headland off the Cotentin Peninsula), and west of Alderney and Ushant islands. Taking into account the reduced ellipticity of the current harmonic M_2 in the majority of sites of interest (Section 3.2, Fig. 9), the tidal current appears thus nearly rectilinear during mean spring conditions, an additional condition required to optimise the exploitation of the tidal kinetic energy resource. Whereas further investigations are required, relying on refined numerical modelling in potential tidal stream sites and integrating the influence of a greater number of harmonic components, these results support the implementation of fixed-orientation (non-yawing) devices.

3.4. Asymmetry of tidal currents

Fig. 13 shows the spatial distributions of asymmetry metrics A_1 (Eq. 9) and A_2 (Eq. 10) in western Brittany and the western English Channel. A close correlation is obtained between both parameters, confirming the reliability of parameter A_1 to characterise the asymmetry of tidal currents from the amplitude and phase of harmonic components M_2 and M_4. At regional scale, numerical results appear consistent with results reported by Robins et al. [7], exhibiting strong tidal asymmetry in the Channel Island Gulf. However, the refined spatial resolution in the present study resolves tidal current asymmetry at the scale of straits, as well as in the vicinity of islands and headlands. Contrasting asymmetries are thus exhibited between sites. The region off the Cotentin Peninsula shows globally weak tidal asymmetry, whereas high values of parameters A_1 and A_2 are obtained in the vicinity of Alderney and coastal headlands, in relation to the formation of tidal residual eddies [42].

Further, the Fromveur Strait is characterised by pronounced tidal current asymmetry. As described elsewhere in the literature [17, 43, 44], this asymmetry is associated with one area experiencing northeast-directed flood-

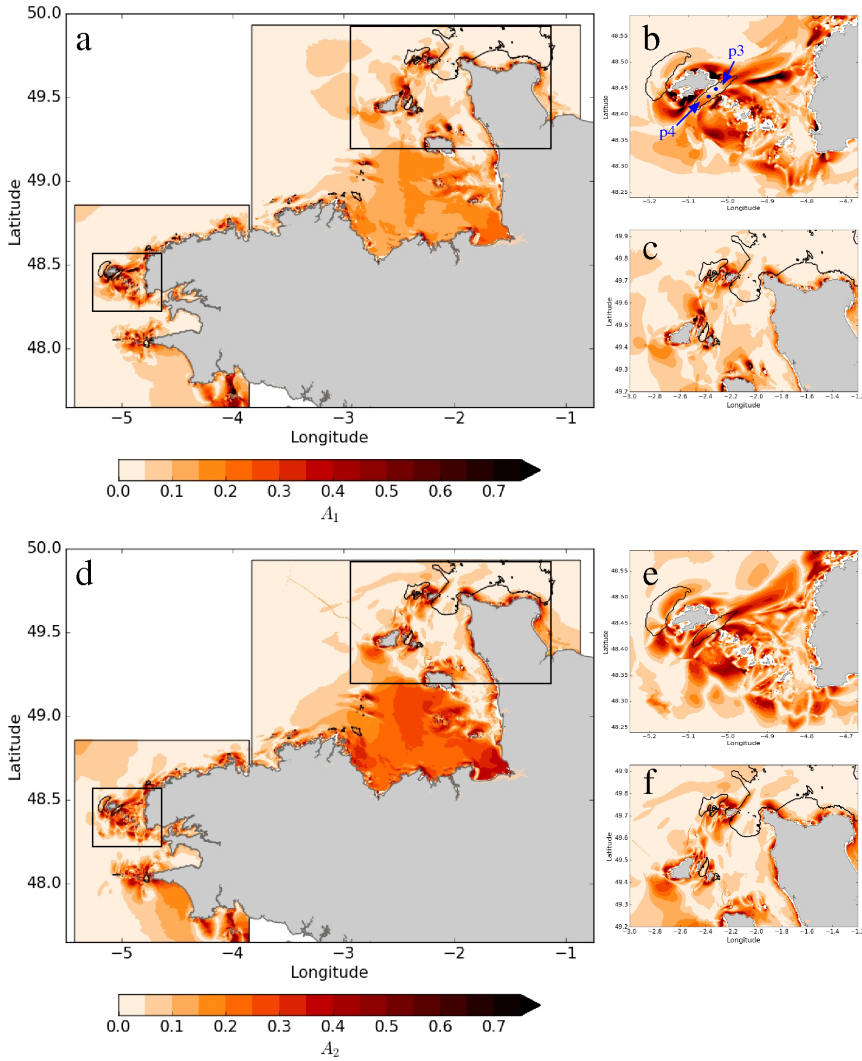

Figure 13: Spatial distribution of parameters A_1 (top) and A_2 (bottom) characterising the asymmetry of tidal currents in (a) coastal domains, with magnified views in (b) the Fromveur Strait and (c) the Alderney Race. The blue circles in (b) show the positions of points p3 and p4 used for the extraction of recomposed currents amplitude and direction in Fig. 14. The black lines delineate potential tidal stream energy sites identified in Fig. 6.

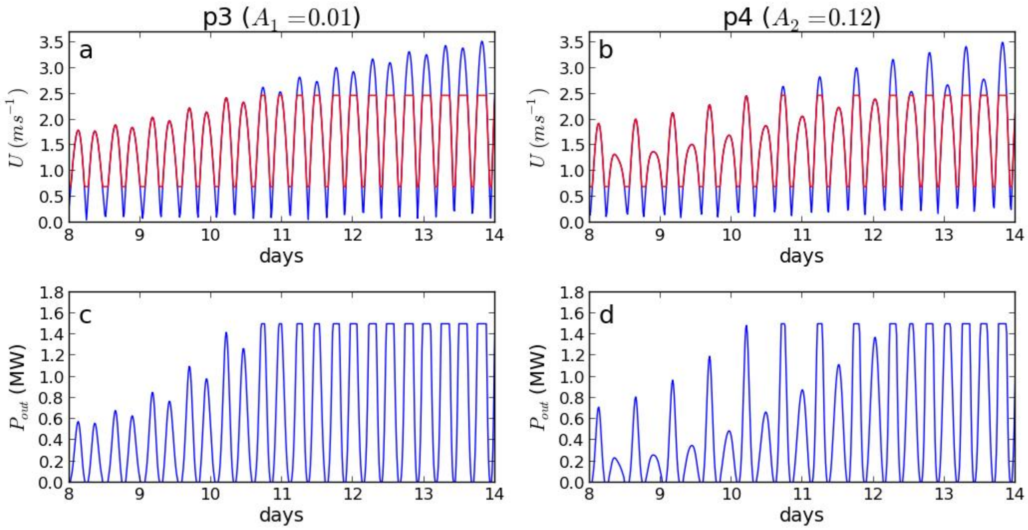

Figure 14: Predicted depth-averaged tidal current speeds U during mean spring-neap conditions and associated generated practical power, P_{out}, based on the 1.5 MW OpenHydro power curve in the central (point p3) and southern (point p4) Fromveur Strait. The red line accounts for the effective tidal velocity which generates power.

dominated flows, and another area experiencing southward ebb-dominated flows. For this region, we confirm the relationship between tidal current asymmetry and the relative phase lag of the M_2 component to M_4, as previously shown from surface velocity measurements by Thiébaut and Sentchev [43], and from numerical simulations by Guillou and Chapalain [44]. The results also confirm the asymmetry in tidal currents off Paimpol-Bréhat reported by Pham and Martin [45].

We extracted depth-averaged tidal velocities from M_2, S_2 and M_4 components, and calculated the associated generated practical power from a hypothetical OpenHydro device at two points in the central (point p3) and southern (point p4) Fromveur Strait (Figs. 13-b and 14). The two locations considered are characterised by similar spring-neap tidal variabilities, with values of parameter $R_{var} \simeq 0.64$. At point p3, the flow is largely symmetrical ($A_1 = 0.01$; Fig. 14-a), with mean spring-neap power estimated at 242 MWh (Fig. 14-c). However, at point p4, the flow is asymmetrical ($A_1 = 0.12$; Fig. 14-b), with mean spring-neap power estimated as 12% less (213 MWh; Fig. 14-d). During the 6-day period from neap to spring conditions, variations of peak practical power were up to 1.0 MW between two consecutive tidal cycles at point p4 (characterised by tidal asymmetry), whereas variations of p3 were restricted to 0.5 MW. This result suggests that fine scale resource assessments are beneficial for device optimisation at array scales. Finally, our results highlight the interest of the Alderney Race, characterised by reduced tidal current asymmetry (Fig. 13), for the exploitation of the tidal kinetic energy resource.

4. Conclusions

A high-resolution tidal harmonic database has been exploited to provide detailed insights into the characteristics of tidal currents and associated power in the coastal waters of France, focusing on western Brittany and the western English Channel – two areas that have strong potential for the exploitation of the tidal kinetic energy resource. The harmonic database has been assessed by comparing recomposed tidal water elevations with observations at a series of harbours along the coasts of France. This evaluation has been extended by comparing recomposed tidal currents with a series of three in-situ ADCP datasets available in the vicinity of principal areas identified for tidal array development. In addition to a map of potential tidal stream energy sites based on current magnitudes and water depths, a method is proposed to exploit, at reduced computational costs, the amplitudes and phases of current harmonic components, and to characterise the spatial and temporal variabilities of the resource. The main outcomes of the present study are as follows:

1. The resource identified in the western English Channel, off the Cotentin Peninsula, has great potential for tidal stream energy – comprising a significant part of the tidal kinetic energy around France. Tidal currents reach 4 $\mathrm{m\,s^{-1}}$ in this region during spring conditions, and the total exploitable surface area is estimated to be 1750 $\mathrm{km^2}$, based on the criteria of mean spring currents greater than 2.0 $\mathrm{m\,s^{-1}}$ and water depths greater than 25 m. The average power density during mean spring tidal conditions varies between 0.9 and 12.4 $\mathrm{kW\,m^{-2}}$, with a mean value estimated at 1.6 $\mathrm{kW\,m^{-2}}$. This accounts for a concentration of tidal stream energy in the Alderney Race, around the Cotentin Peninsula.
2. Strong values of the kinetic power density (over 7 $\mathrm{kW\,m^{-2}}$ during a mean spring tidal cycle) are also obtained in the western area of Alderney (Casquets) and the Fromveur Strait. Other potential locations include areas restricted to 40 $\mathrm{km^2}$, in the Raz of Sein, off Paimpol-Bréhat, to the west of Ushant and to the east of Guernsey (Big Roussel).
3. However, there is significant temporal and spatial variability in the amplitude and direction of tidal stream power. Such variabilities can both reduce the total energy yield, and reduce the consistency of the energy yield over daily-to-fortnightly time scales.
4. The majority of potential tidal stream energy sites investigated here

are characterised by near-rectilinear flows in spring conditions – which favours the installation of fixed-orientation devices.

5. However, some regions show greater spring-neap tidal variability than others (e.g. less variability to the north-east of the Channel Islands and more variability in western Brittany). Sites off the Cotentin Peninsula show, in particular, reduced spring-neap tidal variability, contributing to reduced variations in energy conversion.
6. Tidal currents off the Cotentin Peninsula are largely symmetrical, whereas more pronounced tidal asymmetry occurs off Paimpol-Bréhat, in the western part of the Isle of Ushant and in the Fromveur Strait.

Our results, established using high-spatial resolutions (250 m), provide potential developers with key information to optimise the design and location of kinetic energy converters. The series of metrics reported here may help preliminary assessments of resource variability, both spatially and temporally, particularly useful in areas which have been the subject of a reduced number of investigations of the tidal stream energy resource. However, such resource assessment has naturally to be complemented by refined numerical modelling that integrates, in particular, the complex interactions and modulations of tidal currents with meteorological forcings (wind, waves), and focusing on hydrodynamic characteristics throughout the water column.

Acknowledgements

The authors are particularly grateful to Lucia Pineau-Guillou (Ifremer) for providing access to the tidal harmonic database used in the present investigation (http://www.marc.ifremer.fr/en/produits). In-situ observations and bathymetric data used here were provided by the French navy SHOM ("Service Hydrographique et Océanographique de la Marine"). The treatment of harmonic components was performed on HPC facilities DATARMOR of "Pôle de Calcul Intensif pour la Mer" (PCIM) (http://www.ifremer.fr/HYPERLINK"http://www.ifremer.fr/pcim). The present paper is a contribution to the research program DIADEME ("Design et InterActions des Dispositifs d'extraction d'Energie Marine avec l'Environnement") of the Laboratory of Coastal Engineering and Environment (Cerema, http://www.cerema.fr). Simon Neill and Peter Robins acknowledge the support of the Sêr Cymru National Research Network for Low Carbon, Energy and the Environment (NRN-LCEE), and also the SEACAMS project, which is part-funded by the European Unions Convergence European Regional Development Fund, administered by the Welsh European Funding Office.

References

[1] D. Magagna, A. Uihlein, Ocean energy development in Europe: Current status and future perspectives, International Journal of Marine Energy 11 (2015) 84–104.

[2] Black and Veatch, Phase I. UK tidal-stream energy resource assessment, Tech. rep., London, The Carbon Trust (2004).

[3] H. Tang, K. Qu, G. Chen, S. Kraatz, N. Aboobaker, C. Jiang, Potential sites for tidal power generation: A thorough search at coast of New Jersey, USA, Renewable and Sustainable Energy Reviews 39 (2014) 412–425.

[4] K. Orhan, R. Mayerle, W. W. Pandoe, Assessment of energy production potential from tidal stream currents in Indonesia, Energy Procedia 76 (2015) 7–16.

[5] J. Zheng, P. Dai, J. Zhang, Tidal stream energy in China, Procedia Engineering 116 (2015) 880–887.

[6] Z. Defne, K. A. Haas, H. M. Fritz, L. Jiang, S. P. French, X. Shi, B. T. Smith, V. S. Neary, K. Stewart, National geodatabase of tidal stream power resource in USA, Renewable and Sustainable Energy Reviews 16 (2012) 3326–3338.

[7] P. Robins, S. Neill, M. Lewis, S. Ward, Characterising the spatial and temporal variability of the tidal-stream energy resource over the north-west European shelf seas, Applied Energy 147 (2015) 510–522.

[8] S. Neill, M. Hashemi, M. Lewis, Tidal energy leasing and tidal phasing, Renewable Energy 85 (2016) 580–587.

[9] S. Neill, M. Hashemi, M. Lewis, The role of tidal asymmetry in characterizing the tidal energy resource of Orkney, Renewable Energy 68 (2014) 337–350.

[10] M. Fornerino, C. L. Provost, A model for prediction of the tidal currents in the English Channel, International Hydrographic Review 2 (1985) 143–166.

[11] D. T. Pugh, Tides, Surges and Mean Sea-Level, John Wiley & Sons, Natural Environment Research Council, Swindon, UK, 1987.

[12] M. Piano, S. Neill, M. Lewis, P. Robins, M. Hashemi, A. Davies, S. Ward, M. Roberts, Tidal stream resource assessment uncertainty due to flow asymmetry and turbine yaw misalignment, Renewable Energy 114 (2017) 1363–1375.

[13] G. Egbert, S. Y. Erofeeva, Efficient Inverse Modeling of Barotropic Ocean Tides, Journal of Atmospheric and Oceanic Technology 19 (2002) 183–204.

[14] A. Bahaj, L. Myers, Analytical estimates of the energy yield potential from the Alderney Race (Channel Islands) using maring current energy converters, Renewable Energy 29 (2004) 1931–1945.

[15] J. Thiébot, P. Bailly du Bois, S. Guillou, Numerical modeling of the effect of tidal stream turbines on the hydrodynamics and the sediment transport - Application to the Alderney Race (Raz Blanchard), France, Renewable Energy 75 (2015) 356–365.

[16] N. Guillou, G. Chapalain, S. P. Neill, The influence of waves on the tidal kinetic energy resource at a tidal stream energy site, Applied Energy 180 (2016) 402–415.

[17] N. Guillou, J. Thiébot, The impact of seabed rock roughness on tidal stream power extraction, Energy 112 (2016) 762–773.

[18] D. S. Coles, L. S. Blunden, A. S. Bahaj, Assessment of the energy extraction potential at tidal sites around the Channel Islands, Energy 124 (2017) 171–186.

[19] P. Lazure, F. Dumas, An external-internal mode coupling for a 3D hydrodynamical model for applications at regional scale (MARS)., Advances in Water Resourses 31 (2008) 233–250.

[20] L. Pineau-Guillou, PREVIMER Validation des atlas de composantes harmoniques de hauteurs et courants de marée, Technical Report ODE/DYNECO/PHYSED/2013-03 version 1.0, Ifremer (2013).

[21] R. Le Roy, B. Simon, Réalisation et validation d'un modèle de marée en Manche et dans le Golfe de Gascogne. Application à la réalisation d'un nouveau programme de réduction des sondages bathymétriques, Technical Report 002/03, Service Hydrographique et Océanographique de la Marine (2003).

[22] P. Courtier, J. Thepaut, A. Hollingsworth, A strategy for operational implementation of 4D-VAR, using incremental approach, Quaterly Journal of the Royal Meteorological Society 120 (1994) 1367–1387.

[23] Y. Seity, P. Brousseau, S. Malardel, G. Hello, P. Bénard, F. Bouttier, C. Lac, V. Masson, The AROME-France convective scale operational model, Monthly Weather Review 139 (2011) 976–991.

[24] D. Allain, TUGOm Tidal Toolbox, Documentation available at *ftp://ftp.legos.obs-mip.fr/pub/ecola/tools/ttb.pdf* (2016).

[25] R. Bedard, M. Previsic, O. Siddiqui, G. Hagerman, M. Robinson, Survey and Characterization of Tidal In Stream Energy Conversion (TISEC) Devices, Tech. rep., EPRI (2005).

[26] M. Lewis, S. Neill, P. Robins, M. Hashemi, Resource assessment for future generations of tidal-stream energy arrays, Energy 83 (2015) 403–415.

[27] R. D. Pingree, D. K. Griffiths, Sand transport paths around the British Isles resulting from M_2 and M_4 tidal interactions, Journal of the Marine Biological Association of the United Kingdom 59 (1979) 497–513.

[28] C. T. Friedrichs, D. G. Aubrey, Non-linear tidal distorsion in shallow well-mixed estuaries: a synthesis, Estuarine, Coastal and Shelf Science 27 (1988) 521–545.

[29] L. Pineau-Guillou, PREVIMER Validation des modèles hydrodynamiques 2D des côtes de la Manche et de l'Atlantique, Technical Report ODE/DYNECO/PHYSED/2013-05 version 1.0, Ifremer (2013).

[30] P. Bailly du Bois, F. Dumas, L. Solier, C. Voiseux, In-situ database toolbox for short-term dispersion model validation in macro-tidal seas, application for 2D-model, Continental Shelf Research 36 (2012) 63–82.

[31] C. J. Willmott, On the validation of models, Physical Geography 2 (2) (1981) 219–232.

[32] SHOM, Courants de marée - Mer d'Iroise de l'île Vierge à la pointe de Penmarc'h, Technical Report 560-UJA, Service Hydrographique et Océanographique de la Marine (2016).

[33] Black and Veatch, Phase II. UK tidal-stream energy resource assessment, Tech. rep., London, The Carbon Trust (2005).

[34] A. S. Iyer, S. J. Couch, G. P. Harrison, A. R. Wallace, Variability and phasing of tidal current energy around the United Kingdom, Renewable Energy 51 (2013) 343–357.

[35] L. Biscara, A. Maspataud, T. Schmitt, Présentation de la gamme de MNT bathymétriques pour la modélisation océanographique (projets HOMONIM et TANDEM), in: Colloque merIGéo, 2015.

[36] SHOM, MNT Bathymétrique de la façade Atlantique (Projet HOMONIM), Documentation available at *diffusion.shom.fr/produits/bathymetrie/mnt-facade-atl-homonim.html* (2017).

[37] Black and Veatch, UK tidal current resource and economics, Tech. rep., Commissioned by the Carbon Trust and npower, Project number 121393 (2011).

[38] Environmental Change Institute, Variability in UK marine resources, Technical Report, Commissioned by the Carbon Trust (2005).

[39] C. Christian, R. Vennel, Efficiency of tidal turbine farms, in: Coastal Engineering 2012.

[40] P. Galloway, L. Myers, A. Bahaj, Experimental and numerical results of rotor power and thrust of a tidal turbine operating at yaw and in waves, in: World Renewable Energy Congress 2011 - Marine and Ocean Technology, Linköping, Sweden, 2011.

[41] C. Frost, P. Evans, M. H. an A. Mason-Jones, T. O'Doherty,

D. O'Doherty, The impact of axial flow misalignment on a tidal turbine, Renewable Energy 113 (2017) 1333–1344.

[42] S. Neill, J. Jordan, S. Couch, Impact of tidal energy convertor (TEC) arrays on the dynamics of headland sand banks, Renewable Energy 37 (2012) 387–397.

[43] M. Thiébaut, A. Sentchev, Asymmetry of tidal currents off the Western Brittany coast and assessment of tidal energy resource around Ushant Island, Renewable Energy 105 (2017) 735–747.

[44] N. Guillou, G. Chapalain, Assessing the impact of tidal stream energy extraction on the Lagrangian circulation, Applied Energy 203 (2017) 321–332.

[45] C. Pham, V. Martin, Tidal current turbine demonstration farm in Paimpol-Bréhat (Brittany): tidal characterisation and energy yield evaluation with Telemac, in: Proceedings of the 8th European Wave and Tidal Energy Conference, Uppsala, Sweden, 2009.